Biometals (2012) 25:361–372
DOI 10.1007/s10534-011-9505-7

Cooperative folding of tau peptide by coordination of group IIB metal cations during heparin-induced aggregation

Dan-Jing Yang · Shuo Shi · Tian-Ming Yao · Liang-Nian Ji

Received: 20 June 2011 / Accepted: 1 November 2011 / Published online: 15 November 2011

Abstract The group IIB elements, especially Cd(II) and Hg(II), are increasingly considered as potential environmental neurotoxins. This study demonstrates that the Alzheimer's tau fragment R2, corresponding to the second repeat of the microtubule-binding domain, can bind to Zn(II), Cd(II) and Hg(II). Isothermal titration calorimetry experiments suggest that the most likely coordination site is the thiol group of Cys291, and this is further confirmed by a control experiment using a C291A mutant peptide. Circular dichroism spectrum reveals that the coordination of group IIB cations, especially Hg(II), can induce pronounced conformational conversions in natively unfolded R2, from random coil to other ordered structures. ThS fluorescence assays and electron microscopy indicate that the group IIB cations promote heparin-induced aggregation of R2, giving relatively small R2 filaments. The efficiency in promoting aggregation, as well as inducing conformational conversion, varies strongly with the cation's polarizability. Based on these results, a model is proposed in which the cooperative folding of R2 through cross-bridging of group IIB cations is suggested to be a key factor in promoting aggregation, in addition to the effective neutralization of coulombic charge–charge repulsion by heparin, the poly-anion inducer. Our results provide clues to understanding the potential pathogenic role of group IIB metals in the development of neurofibrillary tangles, a typical hallmark of Alzheimer's disease.

Keywords Aggregation · Conformation · Coordination · Group IIB metals · Tau protein

D.-J. Yang · S. Shi (✉) · T.-M. Yao (✉) · L.-N. Ji
Department of Chemistry, Tongji University, 1239 Siping Road, Shanghai 200092, China
e-mail: shishuo@tongji.edu.cn

T.-M. Yao
e-mail: tmyao@tongji.edu.cn

Introduction

Protein accumulation is a hallmark of many neurodegenerative disorders. In Alzheimer's disease (AD), the protein tau forms intracellular inclusions known as neurofibrillary tangles (NFTs) which are bundles of paired helical filaments (PHFs). Tau protein, a molecule with limited secondary structure in solution (Bergen et al. 2006), nonetheless can be induced to adopt specific conformations in vitro similar to those found in situ (Carmel et al. 1996). The concept of conformational conversion in tau protein as an alternative posttranslational modification in AD has become accepted through various biophysical and biochemical studies (Bergen et al. 2006; Carmel et al. 1996; Ghoshal et al. 2001). The relative contributions of protein refolding and subsequent aggregation of toxic tau are therefore key issues in molecular AD research. Despite several genetic mutations found in AD patients, more than 90% of AD cases are sporadic (Wu et al. 2008). So it is plausible that

environmental exposure may be an etiologic factor in the pathogenesis of AD. Metal ions, which are ubiquitous in the environment, are increasingly believed to be responsible for triggering this pathological positive feedback circle (Bocca et al. 2005; Thompson et al. 1988; Liu et al. 2006).

In this study, the possible involvement of metal ions in tau aggregation is analyzed for the group IIB elements (zinc, cadmium and mercury) and the tau fragment R2, corresponding to the second repeat unit of the microtubule binding domain (residues 275–305: VQIIN KKLDL SNVQS KCGSK DNIKH VPGGGS, according to the longest tau protein).

There is considerable evidence showing that zinc, cadmium and mercury levels in bodies of AD patients are significantly elevated, especially in brain tissues, compared with the normal individuals (Thompson et al. 1988; Mutter et al. 2004; Mutter et al. 2007). Abnormally high levels of zinc have been found in NFTs and senile plaque cores (Thompson et al. 1988; Assaf and Chung 1984). Zinc has been shown to accelerate the aggregation of β-amyloid peptides and tau fragments (Mo et al. 2009; Huang et al. 1997). Cadmium can accumulate with age, and cause acute toxicity, mental retardation, antibiotic resistance, and many other symptoms, even death. It is possible that Cd(II) also hyperactivates the microglia, playing a role in AD (Johnson 2001). Mercury is a known neurotoxin and seems to be absorbed or accumulated in degenerative AD brain more readily than in those of controls (Bocca et al. 2005). Low levels of inorganic mercury are able to cause AD-typical nerve cell deteriorations in vitro and in animal experiments (Mutter et al. 2004, 2007). Therefore, systematic investigations are needed to address the complicated relationship between metals and tau, which in turn would assist in the identification of critical steps in disease progression and the validation of effective therapies.

The second repeat unit of tau plays an important role in the self-aggregation reaction, because it lies in the dense core of Alzheimer-PHFs (Wille et al. 1992; Friedhoff et al. 1998). It can form PHFs more readily than full-length tau isoforms. Such synthetic PHFs resemble those from Alzheimer brain tissue (Jeganathan et al. 2008; Tomoo et al. 2005). This region is of particular interest because the four-repeat and three-repeat tau-isoforms are a direct result of the presence and absence of R2, and it is reported that R2 -included and -deleted tau-isoforms demonstrate a notable difference in their microtubule-binding ability and PHF-formation tendency; The R2 repeat unit exhibits synergistic effect on the aggregation of 4RMBD (Tomoo et al. 2005). This investigation is ultimately aimed at identifying the commonality of metal ions with respect to the ever elusive initial factor(s) that trigger the development of tau aggregation.

Several possible mechanisms for metal-stimulated fibrillation of tau protein can be envisaged. Although many hypotheses favor a role of metal-induced oxidative damage (Sayre et al. 2000; Su et al. 2007; Yamamoto et al. 2002), the simplest would involve direct interactions between tau protein and the metal, leading to structural changes in the tau peptide chain, and resulting in an enhanced propensity to aggregate (Mo et al. 2009; Jiang et al. 2007).

The present study is aimed to probe the potential pathogenic role of group IIB metal cations in the development of NFTs, a typical hallmark of AD. We systematically investigated the interaction between the group IIB cations and tau peptide R2, by various biophysical approaches. We find that tau peptide R2 can bind to the group IIB cations, Zn(II), Cd(II) and Hg(II). The coordination of metal cation, especially Hg(II), induces a conformational conversion on R2 peptide chain. The results suggest that the cooperative folding of R2 through cross-bridging of group IIB cations can have a pronounced impact on tau aggregation.

Materials and methods

Chemicals and peptides

Heparin (average molecular weight, 6000) and Thioflavin S (ThS) were obtained from Sigma Co. The R2 peptide and its mutant (R2-C291A) were chemically synthesized using a solid-phase peptide synthesizer. The samples were obtained in the lyophilized form (including trifluoracetic acid as the counter-ion). The peptides were characterized by mass spectrometry and determined to be $>95.0\%$ pure by reverse-phase HPLC. A solution of R2 was made by dilution to 1 mg/ml with 50 mM Tris–HCl buffer (pH 7.50) before use. The buffer solution contained no reducing reagent such as dithiothreitol (DTT) usually used to block the formation of disulfide bond. All the experiments were conducted in open atmosphere. All the other chemicals were of analytical reagent grade.

ITC measurement

ITC experiments were conducted using a MicroCal VP-ITC unit operating at 37°C. In each experiment, 50 injections (the volume of each injection was 6 μl) of a solution containing metal ions (3,063 μM $ZnCl_2$, or 1,021 μM $CdCl_2$, or 1,021 μM $HgCl_2$) were titrated into a solution of peptide (306 μM, R2 or its mutant R2-C291A) in 50 mM Tris–HCl (pH 7.50) buffer (cell volume = 1.43 ml, stirring speed 290 rpm) using a computer-controlled 310 μl microsyringe. The pH of each solution was checked before starting the analysis. The reference cell was filled with Tris–HCl buffer. Before each experiment, the protein solution was degassed for 2–5 min, to eliminate air bubbles, using the ThermoVac accessory of the microcalorimeter. The first addition started after the baseline stability was achieved. To allow the system to reach equilibrium, a spacing of 240 s between each injection was applied. The feedback mode was set to ''high''. A control experiment was set up, titrating Zn(II), Cd(II), or Hg(II) solution into the buffer under the same conditions. The heat recorded after re-equilibration was due to the reaction occurring within the sample cell. All data were recorded with the software provided by the calorimeter manufacturer. Integrated heat data were fitted using a nonlinear-squares minimization algorithm to a theoretical titration curve, using the MicroCal Origin software and the single set of binding sites model for Zn(II) or Cd(II), and the two sets of binding sites model for Hg(II).

CD measurement

The R2 solution was adjusted to 40.00 μM in 50 mM phosphate buffer, with the pH adjusted to 7.50. All measurements were carried out at 25°C with a JASCO J-810 spectrometer in a cuvette with a 10 mm path length. For each experiment, the measurement from 192 to 252 nm was repeated eight times under N_2 gas flow, and the results were summed. Then the molar ellipticity was determined after normalizing the sample concentration. The same experiment was performed at least three times using the newly prepared samples, and average values were presented in this article.

ThS fluorescence assay of aggregation

The R2 peptide solution was adjusted to a concentration of 15.00 μM using 50 mM Tris–HCl buffer (pH 7.50) containing 10 mM ThS dye. The aggregations were induced by adding (a) heparin (final concentration was 3.80 μM); (b) metal ions [Zn(II), Cd(II) or Hg(II), final concentration were different] and then heparin (final concentration was 3.80 μM) to the solution, and mixing immediately with a pipette prior to fluorescence measurement. The time-dependent fluorescence at 37°C was monitored on an F-7000 fluorescence spectrophotometer (Hitachi) with a quartz cell (2 mm), with excitation at 440 nm and emission at 500 nm. The excitation and emission slit width were both 10 nm. The background fluorescence of the sample was subtracted when needed. For each curve of time-dependent ThS fluorescence, the measurement was performed three times and averaged.

Electron microscope measurement

R2 (15.00 μM) was mixed with (a) heparin (3.80 μM); (b) metal ions [Zn(II), Cd(II) or Hg(II), 15.00 μM] and heparin (3.80 μM), in 50 mM Tris–HCl (pH 7.50). The solution was then incubated at 37°C for 6 h. For negative-staining EM, 600-mesh copper grids were used. A drop of peptide solution and a drop of 2% uranylacetate were placed on the grids. After 2 min, excess fluid was removed from the grids. Negative staining EM was performed using an electron microscope (JEOL JSM-1200EX II) operated at 80 kV.

Results and discussion

Thermodynamics of the binding of group IIB metals to tau fragments R2

Transition metals are frequently recognized as risk factors in neurodegenerative disorders. Among metals, zinc, copper and iron have been most extensively studied so far. Unlike copper and iron, the group IIB metals have completely filled d-orbitals, there is no oxidation reaction possible and the neuro-toxicity can be related directly to the binding to Alzheimer proteins.

To evaluate the affinity of the group IIB metals for tau protein, isothermal titration calorimetry (ITC) experiments were carried out. A typical ITC titration experiment is shown in Fig. 1a–d. The negative peaks of the raw data indicate an exothermic interaction. The heat effects associated with the dilution of the reactants was estimated by titrating metal ion into

buffer solution without R2, and titrating blank buffer into R2/Tris–HCl buffer solution in the same condition. The heats of dilution were subtracted prior to analysis.

Integration of the exothermic peaks yielded the enthalpy change that followed each injection, as shown in Fig. 1e–h. Integrated heat data were fitted using a nonlinear least-squares minimization algorithm. ΔH (reaction enthalpy change in cal mol^{-1}), K_b (binding constant in M^{-1}) and n (number of binding sites) were the fitting parameters. The reaction entropy ΔS was calculated using the equations $\Delta G = -RT \ln K_b$ ($R = 1.9872$ cal mol^{-1} K^{-1}, $T = 298.15$ K) and $\Delta G = \Delta H - T\Delta S$.

For the titrations of both Zn(II) and Cd(II) (Fig. 1e, f), the calorimetric data were best fit to a model assuming a single set of identical sites, with a result of, respectively, (0.52 ± 0.05) and (0.42 ± 0.03) number of binding sites. This indicated that both Zn(II) and Cd(II) bound two R2 fragments per metal ion. Accordingly, we postulate that both Zn(II) and Cd(II) can form a tetrahedral, four-coordinate complex ML_2Cl_2 (L represents tau fragments R2), within a one-step binding process. However, for the titration of Hg(II) (Fig. 1g), the best fit was obtained using the two sets of binding sites model, with the numbers of binding sites, $n_1 = 0.21 \pm 0.001$, $n_2 = 0.25 \pm 0.01$. On the basis of the coordination chemistry of Hg^{2+} (d^{10}), we postulate that Hg(II) binds to R2 with a two-step binding process. The first step, at the molar ratio $n_1 = 0.21 \pm 0.001$, corresponds to the formation of a tetrahedral, four-coordinate complex (HgL_4), while the second step, at the molar ratio $n_2 = 0.25 \pm 0.01$, corresponds to the transition from the complex of HgL_4 to the complex of HgL_2Cl_2 (L represents tau fragments R2).

The thermodynamic parameters for the binding of group IIB cations to tau fragment R2 are summarized in Table 1. The binding process shows a large favorable enthalpic contribution ($\Delta H = -8.46$ to -34.90 kcal mol^{-1}). Among the three cations, Hg(II) possesses the largest heat release, as well as the largest binding constant, along with Cd(II), Zn(II). This trend is consistent with the cation's property as soft acid according to the Pearson's HSAB (hard and soft acids and bases) principle. Considering that the thiol sulfur donor atom is a typical soft Lewis base, we have reason to believe that the very large magnitude of heat release is most likely to be an indication of the formation of

Fig. 1 ITC raw data for titration of **a** $ZnCl_2$ (3,063 μM) into R2 (306 μM), **b** $CdCl_2$ (1,021 μM) into R2 (306 μM), **c** $HgCl_2$ (1,021 μM) into R2 (306 μM), **d** $HgCl_2$ (1,021 μM) into R2-C291A (306 μM), in 50 mM Tris–HCl buffer (pH 7.50) at 37°C; Cell volume: 1.43 ml; Stirring speed: 290 rpm. The integrated heat data, together with the fit of the data obtained with a single set of binding sites model, titration of **e** $ZnCl_2$ (3,063 μM) into R2 (306 μM); **f** $CdCl_2$ (1,021 μM) into R2 (306 μM). The integrated heat data together with the fit of the data obtained with a two sets of binding sites model, titration of **g** $HgCl_2$ (1,021 μM) into R2 (306 μM); **h** $HgCl_2$ (1,021 μM) into R2-C291A (306 μM)

covalent metal-sulfur coordination bond(s), probably between the group IIB metal ion and the thiol sulfur atom of Cys291, because the interaction between soft donor (thiol group of cysteine residue) and soft acceptor (the group IIB cation) is usually strongly exothermic (Ngu-Schwemlein et al. 2009). We also performed a control ITC experiment using Cys291 mutated R2 (R2-C291A), as shown in Fig. 1d, h. All the conditions were the same as those for R2 wild. Unlike the case of R2 wild type, no heat release could be observed in the titration of group IIB metal ions into R2-C291A in 50 mM Tris–HCl buffer (pH 7.50), indicating that the R2 mutant (R2-C291A) did not bind to the group IIB cations. This result clearly indicates that the coordination site involves the Cys291 on the R2 peptide chain. The group IIB cations are known to bind to thiol groups with a high association constant, preferentially forming a stable S-M(II)-S bridge which mimics the physiologically occurring disulfide (S–S) bond in oxidative cellular environment. The disulfide bond is believed to be a very important driving force for tau aggregation (Bhattacharya et al. 2001; Barghorn and Mandelkow 2002).

The binding of Hg(II) to peptide R2 proceeds with two steps. Because of the strong affinity of Hg(II) for R2, and the relatively higher concentrations of R2 than Hg(II) at the beginning of titration, the product in the first step would accordingly resemble a HgL_4 complex, corresponding to the molar ratio of Hg(II) to R2, $n_1 = 0.21 \pm 0.001$ in Fig. 1c. In this step, water and chloride in the reactant, hydrated $HgCl_2$, are completely substituted by R2, with the formation of four Hg–S coordination bonds, showing a very large heat release. A gain in solvent entropy should be observed, however, it will be compensated by a much larger negative change in conformational entropy, and the total entropy change in the first step is still negative. In the second step, with the titration of additional Hg(II) (in the form of hydrated

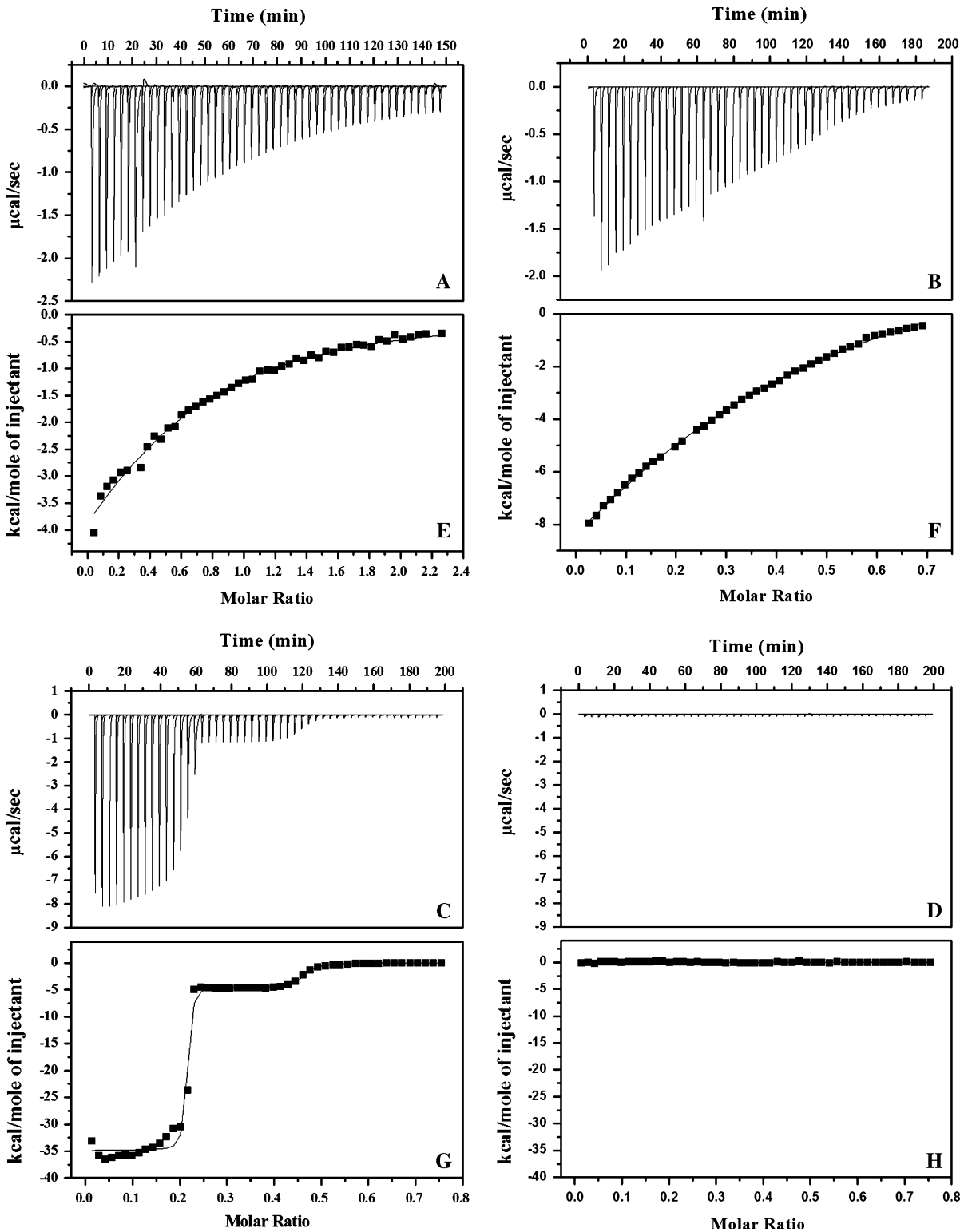
Time (min)
µcal/sec
kcal/mole of injectant
Molar Ratio
A
B
C
D
E
F
G
H

Table 1 Thermodynamic parameters of group IIB metals binding to tau peptide R2 (from ITC data)

Metal ions	ΔH (Kcal mol^{-1})	ΔS(cal mol^{-1} K^{-1})	K_b
Zn(II)	-8.46 ± 0.05	–10.30	$(5.04 \pm 0.56) \times 10^3$
Cd(II)	-11.50 ± 0.15	–16.50	$(3.20 \pm 0.14) \times 10^4$
Hg(II)	(1) -34.90 ± 0.32	(1) -66.6	(1) $(1.03 \pm 0.41) \times 10^{10}$
	(2) -4.50 ± 0.38	(2) 16.10	(2) $(4.89 \pm 1.43) \times 10^6$

$HgCl_2$) into solution, the newly introduced Hg(II) acquires two ligands (R2) from HgL_4 complex, and the complex recomposes to give the HgL_2Cl_2 complex, corresponding to the molar ratio of Hg(II) to R2, $n = n_1 + n_2 = 0.46 \pm 0.01$. In this step, the coordination environment of Hg(II) becomes different. However, it is simply a ligand re-arrangement reaction, no additional coordination bond forms in this process. Therefore, the heat release in the second step is much smaller than that in the first step. In addition, the entropy change in the second step become positive, because there is very little conformational entropy change to compensate the gain in solvent entropy.

In Table 1, the binding constants K_b calculated from the ITC experiment clearly rise with the acceptor's (the group IIB cation) increasing affinity toward sulfur donor: Zn(II) < Cd(II) < Hg(II). Also, it is noted that the rising binding constants are consistent with the increasing heat release in the coordination reaction. In all cases, the binding constant is enthalpically driven and characterized by unfavorable or only slightly favorable entropy changes. Compared with the binding of Cu(II) to tau protein (Soragni et al. 2008), where the dissociation constant $K_d = 0.5$ μM for full-length tau protein, the binding of Hg(II) to R2 is very strong, while the binding of Zn(II) or Cd(II) to R2 is relatively weak.

Effects of group IIB metals coordination on the conformation of R2 examined by CD spectrum

Since the conformational conversion is widely believed to be the central event in protein aggregation (Bergen et al. 2006; Carmel et al. 1996; Ghoshal et al. 2001), there is a clear need for detailed experimental evidence to resolve the issue of what really happens in the stages of coordination by group IIB metals. The CD spectrum in far-UV region, which could provide reasonable estimate of secondary structure, was thus employed.

In Fig. 2, the soluble tau construct R2 was dominated by random coil structure in the unbound state, consistent with earlier observations (Jeganathan et al. 2008). This was characterized by a negative peak around 198 nm. With the stepwise titration of the group IIB cation into R2 solution, the signal at about 198 nm gradually decreased, suggesting a loss of random coil conformation.

For titrations of Zn(II) and Cd(II) (Fig. 2a, b), the decrease of the CD signal at 198 nm was rather small, and not accompanied by any additional spectral change elsewhere. Therefore, at the present stage, the CD experiment could only give information that Zn(II) or Cd(II) induced a partial elimination of the random coil structure, probably because the peptide chain gradually lost its freedom of rotation or folding, as Zn(II) or Cd(II) coordinating with it.

However, for the titration of Hg(II) (Fig. 2c), a drastic decrease of the CD signal at 198 nm was accompanied by the emergence of a positive signal at about 210 nm. This positive signal is assigned to β-turn structure (Greenfield 1996; Kelly et al. 2005). This change in the CD spectrum clearly suggests a conformational conversion from random coil to β-turn structure, a folding of R2 peptide chain induced by Hg(II) coordination, which is believed to be a key factor for tau aggregation.

As shown in Fig. 2E, the CD signal at 198 nm was analyzed in terms of the molar ratios of metal to R2. Clearly it was observed that the conformation of R2 was altered in different ways by different metals. The conformational conversion induced by Hg(II) was most pronounced. It is worthy of note that the efficiencies of group IIB cations to induce conformational conversion are correlated with their increasing binding constant, as shown in Table 1.

Many efforts have been directed toward determining the fundamental forces involved in protein folding induced by metal coordination. A simplified view of the forces influencing overall protein structure suggests involvement of neutralization of charge on peptide chain, especially for some negatively charged proteins (Uversky et al. 2001). However, the present situation is different, because peptide R2 is positively

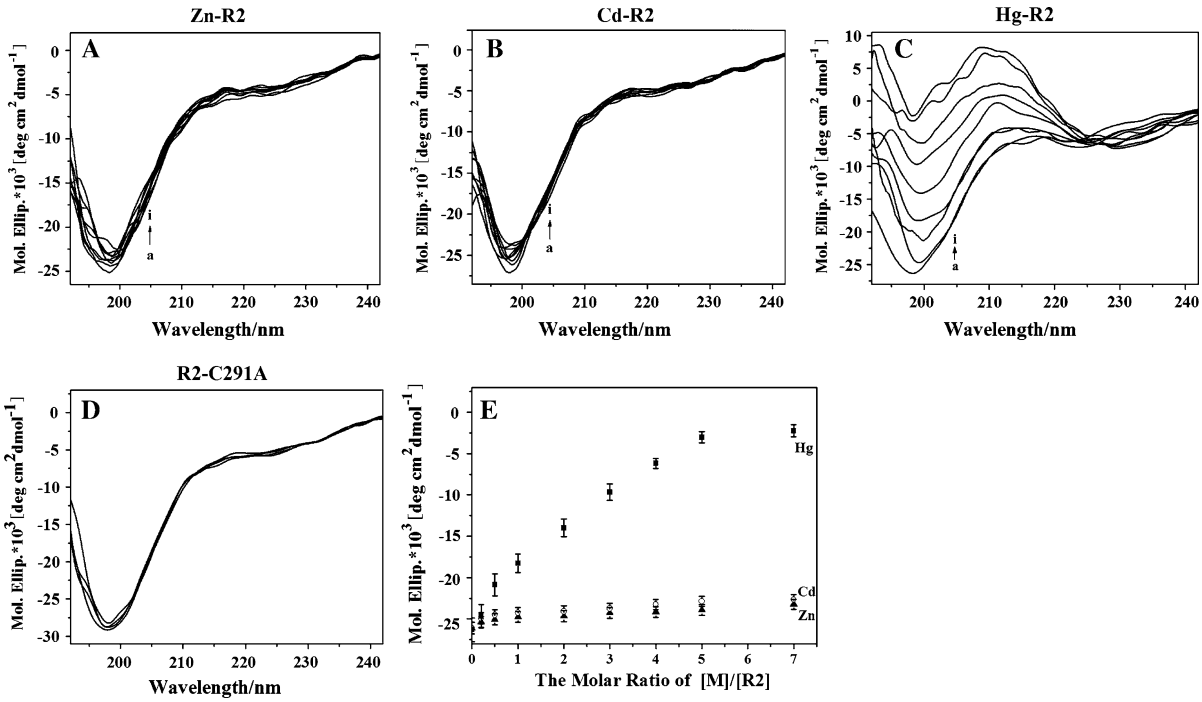

Fig. 2 CD spectra of R2 with different amounts of **a** $ZnCl_2$; **b** $CdCl_2$; **c** $HgCl_2$. The sample solutions are 40.00 μM R2 mixed with the molar ratio of [M(II)]/[R2] (from a–i): 0.00, 0.20, 0.50, 1.00, 2.00, 3.00, 4.00, 5.00 and 7.00 in phosphate buffer (pH 7.50). **d** CD spectra of R2-C291A with group IIB metal ions. The sample solutions are 40.00 μM R2-C291A mixed with the molar ratio of [M]/[R2-C291A] = 0.00; [$ZnCl_2$]/[R2-C291A] = 7.00; [$CdCl_2$]/[R2-C291A] = 7.00; and [$HgCl_2$]/[R2-C291A] = 7.00, respectively. **e** Plots of the CD signals at 198 nm versus the molar ratio of [$ZnCl_2$]/[R2], [$CdCl_2$]/[R2] and [$HgCl_2$]/[R2]

charged. The above data demonstrate that the conformational conversion is specifically due to the coordination of group IIB cations with peptide R2. This was further confirmed by a control experiment, using a cysteine to alanine mutated R2 peptide (R2-C291A), as shown in Fig. 2d. It was noted that the CD spectra of R2-C291A had no major difference, whether the group IIB cations were present in solution or not.

A conformational conversion surrounding the metal coordination site can form a network, whose accumulated effect in a large molecule can be quite significant (Nelson and Cox 2004). Both of the geometrical preferences of the metal and the allosteric organization of peptide are contributing to the final structure.

Impacts of group IIB metals coordination on the heparin-induced aggregation of R2 examined by ThS fluorescence assay and electron microscopy

Because the kinetics of the reaction can shed light on the mechanism of polymerization, the time-dependence of polymer formation was monitored using thioflavin S (ThS) fluorescence. Without metal ions, the time profile of the heparin-induced aggregation of R2 showed a very smooth increase in ThS fluorescence (curve a in Fig. 3a–c), the same pattern as reported earlier (Minoura et al. 2004). The impact of Zn(II), Cd(II) or Hg(II) on the aggregation reaction of R2 was then evaluated. When Zn(II) (Fig. 3a), Cd(II) (Fig. 3b) or Hg(II) (Fig. 3c) was gradually added into the solution, the ThS fluorescence intensity increased while, at the same time, the long lag time was reduced.

Kinetic parameters were determined by fitting ThS fluorescence intensity versus time to a sigmoidal equation (Mo et al. 2009),

$$F = F_0 + (A + \mathrm{ct})/\{1 + \exp[k(t_\mathrm{m} - \mathrm{t})]\} \quad (1))$$

where F is the fluorescence intensity, i is the rate constant for the growth of fibrils, and t_m is the time to 50% of maximal fluorescence. The initial baseline during the lag time is described by F_0. The final baseline after the growth phase has ended is described by A + ct. The lag time is calculated as $t_\mathrm{m}-2/\mathrm{k}$.

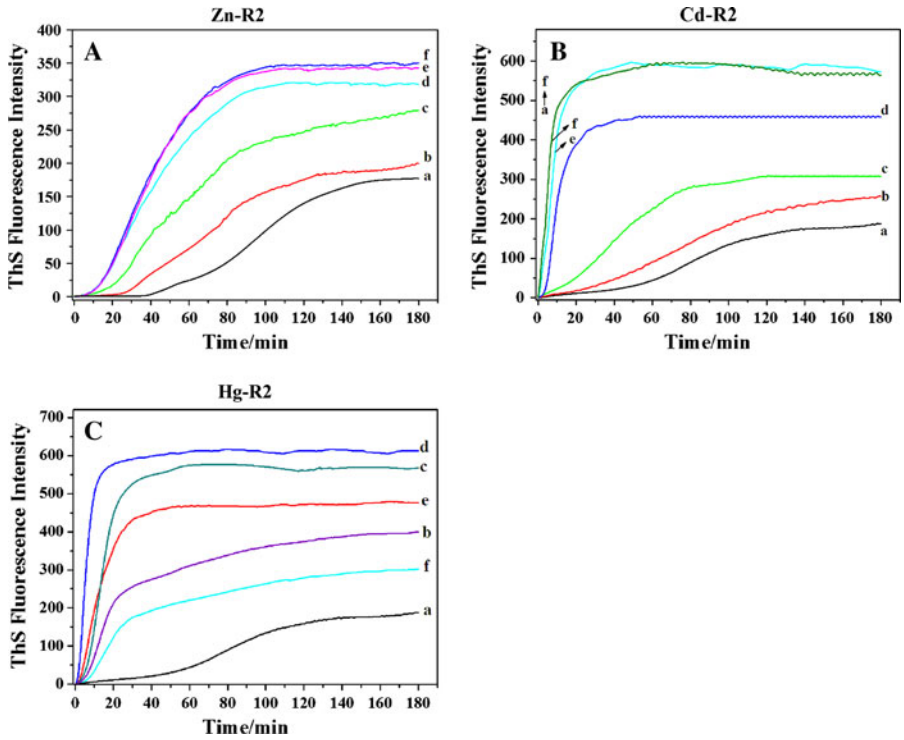

Fig. 3 Time-dependent profiles of R2 aggregation monitored by ThS fluorescence at 37°C with different molar ratios of **a** [$ZnCl_2$]/[R2] (from a to f): 0.00, 0.50, 1.00, 1.20, 1.50 and 2.00; **b** [$CdCl_2$]/[R2] (from a–f): 0.00, 0.10, 0.20, 0.40, 0.80 and 1.20; **c** [$HgCl_2$]/[R2] (from a–f): 0.00, 0.20, 0.40, 0.50, 0.75 and 0.90. R2 was adjusted to the final concentration of 15.00 μM using 50 mM Tris–HCl buffer (pH 7.50), containing 10 mM ThS dye, and different amount of metal ions. The aggregations were induced by adding heparin (final concentration was 3.80 μM) prior to fluorescence measurement

The kinetic parameters of heparin-induced aggregation of R2 in presence of the group IIB metals (at the optimum molar ratios), monitored by ThS fluorescence at 37°C, are summarized in Table 2. The rate constants of R2 aggregation promoted by Zn(II), Cd(II) and Hg(II) are, respectively, 76.53, 370.49 and 545.51. These results indicate that all the group IIB cations promote heparin-induced aggregation of R2. It is worthy of note that the rate constants of R2 aggregation reaction promoted by different cations increase in the series: Zn(II) < Cd(II) < Hg(II), which is also consistent with the trend of increasing affinities of metal to R2.

The aggregate products of R2 were then examined by electron microscopy. Fig. 4 illustrates the morphologies of the resulting filaments in heparin-induced aggregation reaction under conditions, with or without the group IIB metals. Both the aggregate products appear to be straight and long. Similar morphology implies that group IIB metal cations do not alter the overall molecular arrangement within the filaments. However, the filaments become thinner, from ~15 nm (Fig. 4a) to 10–6 nm (Fig. 4b–d) in width, if Zn(II), Cd(II) and Hg(II) are introduced respectively into the system. This may be an implication that group IIB cations are able to accelerate heparin-induced aggregation of R2 from nucleation step (Mo et al. 2009; Tomoo et al. 2005). That is, the intermolecular linkage by S-M(II)-S coordination bridge facilitates the dimerization and/or oligomerization of tau monomers, and the resulting tau dimers and/or oligomers are believed to be building blocks to construct the core of filament.

Table 2 Kinetic parameters of R2 aggregation with/without group IIB metals monitored by ThS fluorescence at 37°C

	$k(10^{-3}\ min^{-1})$	t_m(min)	Lag time(min)
R2	50.80 ± 0.14	81.16 ± 0.07	41.73
Zn(II)	76.53 ± 0.51	40.23 ± 0.10	14.10
Cd(II)	370.49 ± 6.37	5.63 ± 0.05	0.22
Hg(II)	545.51 ± 9.28	3.76 ± 0.05	0.09

Kinetic parameters of R2 aggregation with group metals were calculated at the optimum molar ratio of [M(II)]/[R2]; k the rate constant for the growth of fibrils; t_m: the time to 50% of maximal fluorescence; *Lag time* calculated as t_m–2/k

Hypothetical mechanism of heparin-induced aggregation of R2 promoted by group IIB cations

How can the current data be related with the intrinsic properties of group IIB metals? In Fig. 5, we have

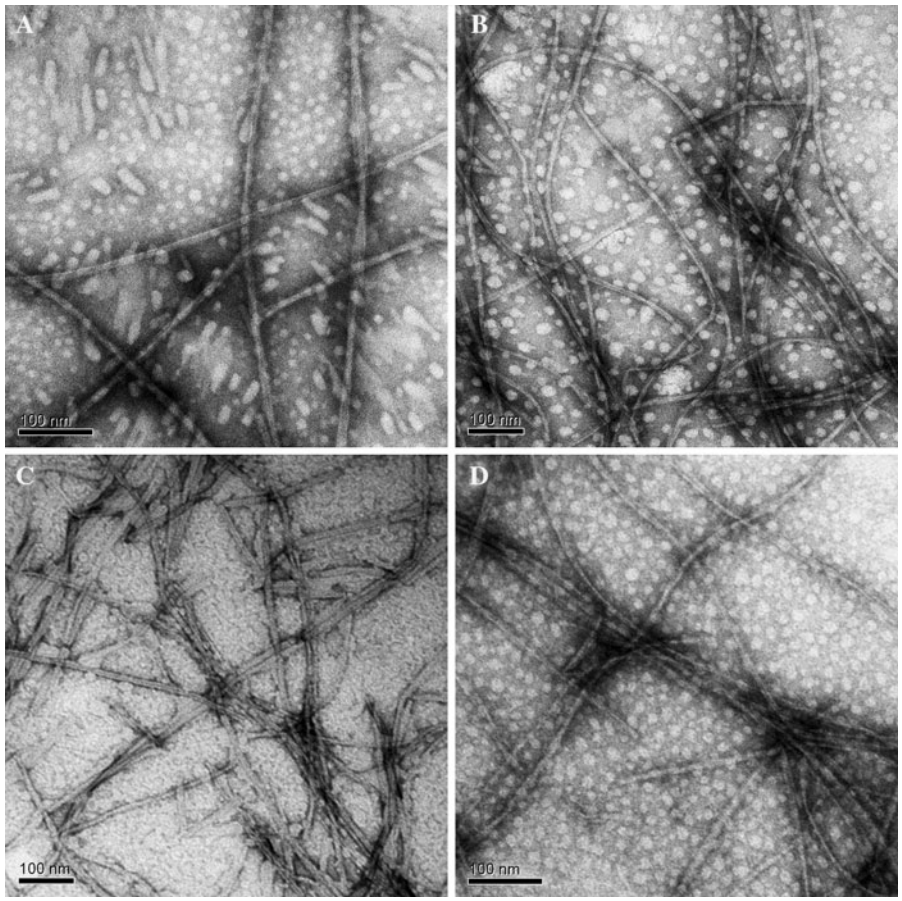

Fig. 4 The EM images of the resulting R2 filaments. Aggregation of R2 (15 μM) was induced by heparin (3.80 μM) in 50 mM Tris–HCl buffer (pH 7.50). All the samples are incubated at 37°C for 6 h. **a** without metal cation; **b** with Zn(II) (15 μM); **c** with Cd(II) (15 μM); **d** with Hg(II) (15 μM)

drawn a comparison between the polarizabilities (Massaro 2002) of group IIB cations and the values of lgK_b (K_b is the binding constant of group IIB cation to R2), along with the R2 conformational conversion induced by group IIB cations (calculated from the decrease of CD signal at 198 nm), the rate constants of R2 aggregation reaction promoted by group IIB cations. It is known that the polarizability and/or polarizing power of IIB group metals increase in the sequence, Zn(II) < Cd(II) < Hg(II), attributable to the electronic configuration and nuclear charge. As expected we find that the binding constant increases in a similar pattern as the cation's polarizability, consistent with Pearson's HSAB principle. The preferential binding of group IIB cations by soft Lewis bases is due to mutual polarization of the cation (Zn^{2+}, Cd^{2+} or Hg^{2+}) and its ligands (Cys291).

For any protein polymerization system, it is of fundamental importance to understand the molecular mechanism that regulates the process. Based on the current data, a unified scheme has been proposed concerning the mechanism of the heparin-induced aggregation of R2 promoted by IIB group cations (Fig. 6). In general, the R2 peptide chain is natively unstructured prior to metal binding. Because of its affinity for IIB group cations, R2 coordinates through the side chain of Cys291 with these cations whenever introduced into solution, giving a four-coordinated, tetrahedral complex MCl_2L_2 (M = Zn(II), Cd(II) or Hg(II); L = R2), which is an intermediate of the

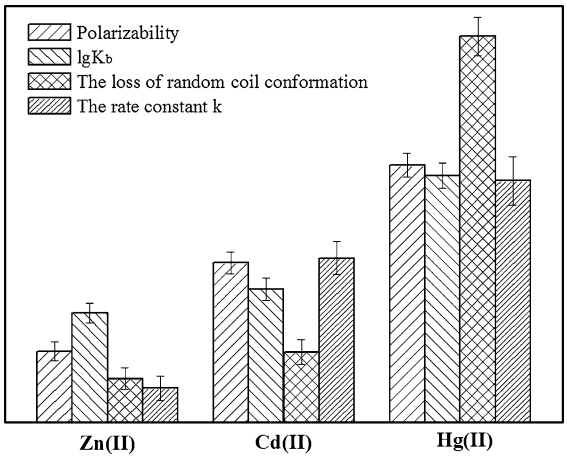

Fig. 5 The comparison between the polarizabilities of group IIB cations and the values of lgK_b (K_b is the binding constant of group IIB cation to R2), along with the decrease of CD signal at 198 nm resulting from the titration of group IIB metals (280 μM) into R2 (40 μM), the rate constants of R2 aggregation reaction promoted by group IIB cations at the optimum molar ratio of [M(II)]/[R2]

aggregation reaction. Cross-linked by group IIB cations, R2 undergoes a dimerization process through a stable -S-M(II)-S- bridge which mimics the physiologically occurring disulfide (S–S) bond in oxidative cellar environment. Concurrently, the overall R2 peptide chain undergoes a conformational conversion to adapt to the favorable coordination geometry of group IIB cations, for example, in the case of Hg(II) ions, specifically from random coil to β-turn structure. This step, termed the nascent stage of folding, is responsible for the initial collapse of the polypeptide chain into a compact structure. However, due to a high net charge near physiological pH, the resulting compact structure experiences unfavorable electrostatic repulsion. Under these conditions, negatively charged molecules such as heparin can help offset the electrostatic repulsion, thereby reinforcing the entire network around the metal coordination sphere. Overall the aggregation of R2 appears to be facilitated by supramolecular forces, which organize flexible

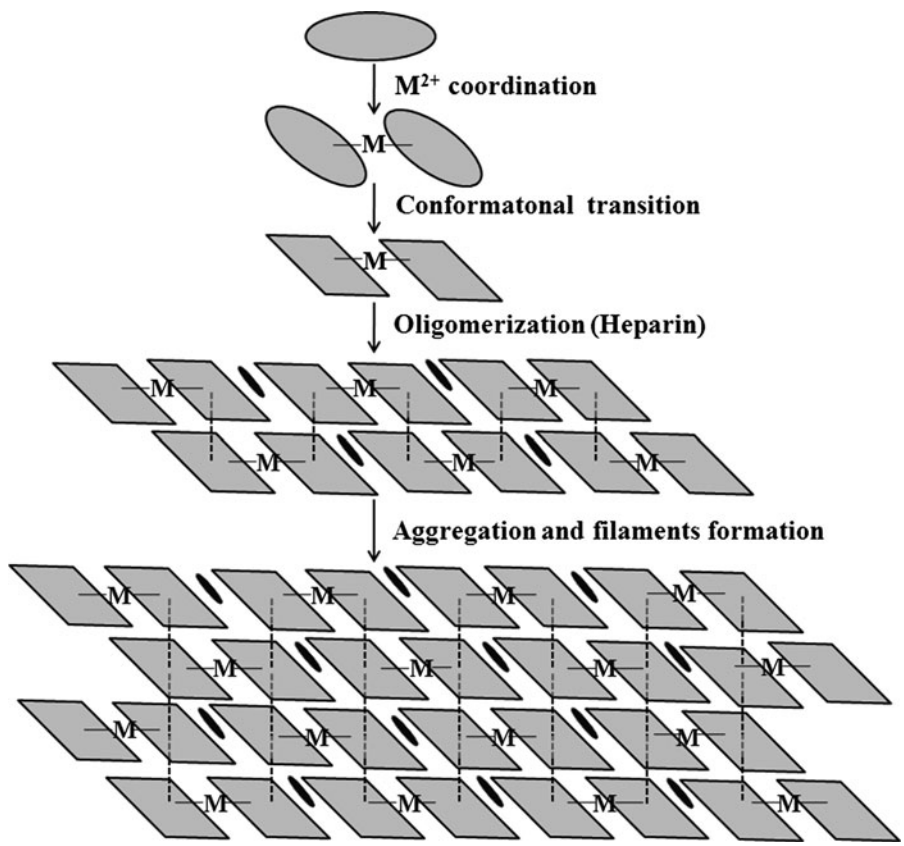

Fig. 6 Hypothetical mechanisms of the heparin-induced aggregation of R2 promoted by group IIB cations. Ellipses represent the natural R2; parallelograms represent R2 after conformational conversion; M represents Zn(II), Cd(II) or Hg(II); and the rods represent polyanion, for example heparin

peptides, and result in the allosteric formatives of the large complex.

Acknowledgments This work was supported by the National Natural Science Foundation of China (Nos. 20871094, 20901060, 20472065). We thank the support of the opening foundation of the MOE key laboratory of Bioinorganic and Synthetic Chemistry, Sun Yet-Sen University.

References

Assaf SY, Chung SH (1984) Release of endogenous Zn^{2+} from brain tissue during activity. Nature 308:734–736

Barghorn S, Mandelkow E (2002) Toward a unified scheme for the aggregation of tau into Alzheimer paired helical filaments. Biochemistry 41:14885–14896

Bergen M, Barghorn S, Jeganathan S, Mandelkow EM, Mandelkow E (2006) Spectroscopic approaches to the conformation of tau protein in solution and in paired helical filaments. Neurodegenerative Dis 3:197–206

Bhattacharya K, Rank KB, Evans DB, Sharma SK (2001) Role of cysteine-291 and cysteine-322 in the polymerization of human tau into Alzheimer-like filaments. Biochem Biophy Res Co 285:20–26

Bocca B, Forte G, Petrucci F, Pino A, Marchione F, Bomboi G, Senofonte O, Giubilei F, Alimonti A (2005) Monitoring of chemical elements and oxidative damage in patients affected by Alzheimer's disease. Ann Ist Super Sanita 41:197–203

Carmel G, Mager EM, Binder LI, Kuret J (1996) The structural basis of monoclonal antibody Alz50's selectivity for Alzheimer's disease pathology. J Biol Chem 271:32789–32795

Friedhoff P, Schneider A, Mandelkow EM, Mandelkow E (1998) Rapid assembly of Alzheimer-like paired helical filaments from microtubule-associated protein tau monitored by fluorescence in solution. Biochemistry 37: 10223–10230

Ghoshal N, García-Sierra F, Fu Y, Beckett LA, Mufson EJ, Kuret J, Berry RW, Binder LI (2001) Tau-66: evidence for a novel tau conformation in Alzheimer's disease. J Neurochem 77:1372–1385

Greenfield NJ (1996) Methods to estimate the conformation of proteins and polypeptides from circular dichroism data. Anal Biochem 235:1–10

Huang X, Atwood CS, Moir RD, Hartshorn MA, Vonsattel JP, Tanzi RE, Bush AI (1997) Zinc-induced Alzheimer's Abeta1–40 aggregation is mediated by conformational factors. J Biol Chem 272:26464–26470

Jeganathan S, von Bergen M, Mandelkow EM, Mandelkow E (2008) The natively unfolded character of tau and its aggregation to Alzheimer-like paired helical filaments. Biochemistry 47:10526–10539

Jiang LF, Yao TM, Zhu ZL, Wang C, Ji LN (2007) Impacts of Cd(II) on the conformation and self-aggregation of Alzheimer's tau fragment corresponding to the third repeat of microtubule-binding domain. Biochim Biophys Acta 1774:1414–1421

Johnson S (2001) Gradual micronutrient accumulation and depletion in Alzheimer's disease. Med Hypotheses 56: 595–597

Kelly SM, Jess TJ, Price NC (2005) How to study proteins by circular dichroism. Biochim Biophy Acta 1751:119–139

Liu GJ, Huang WD, Moir RD, Vanderburg CR, Lai B, Peng ZC, Tanzi RE, Rogers JT, Huang XD (2006) Metal exposure and Alzheimer's pathogenesis. J Struct Biol 155:45–51

Massaro EJ (2002) Handbook of neurotoxicology. Humana Press Inc, Totowa

Minoura K, Yao TM, Tomoo K, Sumida M, Sasaki M, Taniguchi T, Ishida T (2004) Different associational and conformational behaviors between the second and third repeat fragments in the tau microtubule-binding domain. Eur J Biochem 271:545–552

Mo ZY, Zhu YZ, Zhu HL, Fan JB, Chen J, Liang Y (2009) Low micromolar zinc accelerates the fibrillization of human tau via bridging of Cys-291 and Cys-322. J Biol Chem 284:34648–34657

Mutter J, Naumann J, Sadaghiani C, Schneider R, Walach H (2004) Alzheimer disease: mercury as pathogenetic factor and apolipoprotein E as a moderator. Neuro Endocrinol Lett 25:331–339

Mutter J, Naumann J, Schneider R, Walach H (2007) Mercury and Alzheimer's disease. Fortschr Neurol Psychiatr 75:528–538

Nelson DL, Cox MM (2004) Lehninger principles of biochemistry. W.H. Freeman, New York

Ngu-Schwemlein M, Merle JK, Healy P, Schwemlein S, Rhodes S (2009) Thermodynamics of the complexation of Hg(II) by cysteinyl peptide ligands using isothermal titration calorimetry. Thermochimica Acta 496:129–135

Sayre LM, Perry G, Harris PLR, Liu Y, Schubert KA, Smith MA (2000) In situ oxidative catalysis by neurofibrillary tangles and senile plaques in Alzheimer's disease: a central role for bound transition metals. J Neurochem 74:270–279

Soragni A, Zambelli B, Mukrasch MD, Biernat J, Jeganathan S, Griesinger C, Ciurli S, Mandelkow E, Zweckstetter M (2008) Structural characterization of binding of Cu(II) to tau protein. Biochemistry 47:10841–10851

Su XY, Wu WH, Huang ZP, Hu J, Lei P, Yu CH, Zhao YF, Li YM (2007) Hydrogen peroxide can be generated by tau in the presence of Cu(II). Biochem Biophy Res Co 358: 661–665

Thompson CM, Markesbery WR, Ehmann WD, Mao YX, Vance DE (1988) Regional brain trace-element studies in Alzheimer's disease. Neurotoxicology 9:1–7

Tomoo K, Yao TM, Minoura K, Hiraoka S, Sumida M, Taniguchi T, Ishida T (2005) Possible role of each repeat structure of the microtubule-binding domain of the tau protein in in vitro aggregation. J Biochem 138:413–423

Uversky VN, Li J, Fink AL (2001) Metal-triggered structural transformations, aggregation, and fibrillation of human alpha-synuclein. A possible molecular NK between Parkinson's disease and heavy metal exposure. J Biol Chem 276:44284–44296

Wille H, Drewes G, Biernat J, Mandelkow EM, Mandelkow E (1992) Alzheimer-like paired helical filaments and antiparallel dimers formed from microtubule-associated protein tau in vitro. J Cell Biol 118:573–584

Wu JF, Basha MR, Zawia NH (2008) The environment, epigenetics and amyloidogenesis. J Mol Neurosci 34:1–7

Yamamoto A, Shin RW, Hasegawa K, Naiki H, Sato H, Yoshimasu F, Kitamoto T (2002) Iron (III) induces aggregation of hyperphosphorylated tau and its reduction to iron (II) reverses the aggregation: implications in the formation of neurofibrillary tangles of Alzheimer's disease. J Neurochem 82:1137–1147